Published in final edited form as:
*Pain*. 2010 December ; 151(3): 633–643. doi:10.1016/j.pain.2010.08.030.

# Persistent Inflammation Alters the Density and Distribution of Voltage-Activated Calcium Channels in Subpopulations of Rat Cutaneous DRG neurons

**Shao-Gang Lu**[1], **Xiu-Lin Zhang**[1], **Z. David Luo**[4], and **Michael S. Gold**[1,2,3]

[1] Department of Medicine, Division of Gastroenterology, Hepatology and Nutrition, University of Pittsburgh, Pittsburgh, PA 15213

[2] Department of Neurobiology, University of Pittsburgh, Pittsburgh, PA 15213

[3] Pittsburgh Center for Pain Research, University of Pittsburgh, Pittsburgh, PA 15213

[4] Department of Anesthesiology & Perioperative Care, School of Medicine, University of California, Irvine, Irvine, CA 92697

## Abstract

The impact of persistent inflammation on voltage-activated $Ca^{2+}$ channels in cutaneous DRG neurons from adult rats was assessed with whole cell patch clamp techniques, sqRT-PCR and Western blot analysis. Inflammation was induced with a subcutaneous injection of complete Freund's adjuvant (CFA). DiI was used to identify DRG neurons innervating the site of inflammation. Three days after CFA injection, high threshold $Ca^{2+}$ current (HVA) density was significantly reduced in small and medium, but not large diameter neurons, reflecting a decrease in N-, L- and P/Q-type currents. This decrease in HVA-current was associated with an increase in mRNA encoding the $\alpha 2\gamma 1$-subunit complex, but no detectable change in N-type subunit ($Ca_V2.2$) mRNA. An increase in both $\alpha 2\gamma 1$ and $Ca_V2.2$ protein was detected in the central nerves arising from L4 and L5 ganglia ipsilateral to the site of inflammation. In current clamp experiments on small and medium diameter cutaneous DRG neurons from naïve rats, blocking ~40% of HT-VGCC with $Cd^{2+}$ (5 μM), had opposite effects on subpopulations of cutaneous DRG neurons (increasing excitability and action potential duration in some and decreasing excitability in others). The alterations in the density and distribution of voltage-activated $Ca^{2+}$ channels in subpopulations of cutaneous DRG neurons that develop following CFA injection should contribute to changes in sensory transmission observed in the presence of inflammation.

### Keywords

pain; nociceptor; primary afferent; retrograde tracer; protein trafficking; sensitization

Corresponding Author: Michael S. Gold, PhD, Department of Medicine, University of Pittsburgh, 3500 Terrace Street Rm E1440 BST, Pittsburgh, PA 15213, Phone (412) 383-5367, Fax: (412) 383-8663, msg22@pitt.edu.

## 1. Introduction

Tissue inflammation is associated with ongoing pain and hyperalgesia that reflects, at least in part, an increase in afferent input to the central nervous system. A number of ionic mechanisms have been identified that may contribute to this increase in input including changes in both voltage-activated $Na^+$ [3] and $K^+$ [41,16,26] currents. There are several reasons to suggest, however, that an increase in voltage-activated $Ca^{2+}$ currents may contribute to the inflammation-induced increase in afferent input, as well. First, an increase in low-threshold, or T-type voltage-activated (LVA) $Ca^{2+}$ currents in peripheral afferent terminals is associated with a decrease in nociceptive threshold [8,29]. Second, inflammatory injuries are associated with an increase in α-subunit protein thought to underlie P/Q-type high threshold voltage-activated (HVA) $Ca^{2+}$ currents [49]. Third, persistent inflammation results in an increase in $Ca^{2+}$ dependent transmitter release from primary afferents [28,43]. Fourth, inflammation and nerve injury appear to have opposite effects on the expression of several ion channels [3] and nerve injury results in a decrease in both HVA- [4,27,1,39] and LVA- [38] $Ca^{2+}$ currents in primary afferents. Nevertheless, despite evidence suggesting that persistent inflammation may result in an increase in voltage-activated $Ca^{2+}$ currents in primary afferents, the impact of persistent inflammation on $Ca^{2+}$ currents in these neurons has not been directly studied. Therefore, the purpose of the present study was to test the hypothesis that the persistent inflammation is associated with an increase in $Ca^{2+}$ currents in nociceptive afferents.

$Ca^{2+}$ currents were assessed in acutely isolated somata of cutaneous afferents from adult rats with whole cell patch clamp techniques. To identify the subpopulation of neurons directly impacted by persistent inflammation, afferents innervating the glabrous skin of the hindpaw were identified with the retrograde tracer, DiI. DRG neurons were studied from naïve rats and from rats in which inflammation had been induced at the site of the DiI injection with complete Freund's adjuvant (CFA). Semi-quantitative reverse-transcriptase polymerase chain reaction (sqRT-PCR) and western blot analysis were used to assess the basis for observed changes in current density. Finally, to assess the impact of inflammation-induced changes in $Ca^{2+}$ currents on the excitability of sensory neurons, the impact of pharmacological inhibition of $Ca^{2+}$ currents was assessed in current clamp.

## 2. Materials and methods

### 2.1. Rats

Adult (240–340g) male Sprague-Dawley rats (Harlan, Indianapolis, IN) were used for this study. Rats were housed in either the University of Maryland Dental School, or the University of Pittsburgh animal facility in groups of two or three on a 12:12 light dark schedule. Food and water are available *ad lib.* All experiments were approved by both the University of Maryland Dental School and the University of Pittsburgh Institutional Animal Care and Use Committees and performed in accordance with National Institutes of Health guidelines as well as guidelines established by the International Association of the Study of Pain for the use of laboratory animals in research. Rats were deeply anesthetized for tissue labeling, inflammation and harvest of DRG. The depth of anesthesia was assessed by monitoring for the presence or absence of corneal reflexes and withdrawal responses from noxious pinch of the hindpaw. Respiration rate was also monitored. Supplemental anesthesia was administered until animals were areflexive. Following tissue harvest, rats were killed by decapitation.

### 2.2. Labeling of DRG neurons innervating the glabrous skin of the hindpaw

DRG neurons giving rise to innervation of the glabrous skin of the hindpaw were labeled with the retrograde tracer DiI (1,1'-dioctadecyl-3,3,3',3'-tetramethylindocarbo-cyanine perchlorate (Invitrogen, Carlsbad, CA)). Labeling was performed as previously described [36]. DiI was

dissolved in DMSO (170 mg/ml, Sigma-Aldrich, St. Louis, MO) and diluted 1:10 in 0.9% sterile saline. Diluted dye (10 μl total injected over an area ~5 $mm^2$) was injected subcutaneously with a 30 g injection needle under anesthesia induced by 5% isoflurane (Abbott Laboratories, North Chicago, IL, USA) and maintained with 1.5% isoflurane. Injections were made bi-laterally. DiI-labeled neurons were easily identified under epifluorescence illumination with a Texas-red filter set.

To assess the spread of DiI in the hindpaw, and therefore the subpopulations of DRG neurons likely to be retrogradely labeled with DiI, we analyzed the labeling pattern in the feet of 5 rats used for electrophysiological studies. Two additional rats were studied with an injection of two tracers (DiO (3,3'-dioctadecyloxacarbocyanine perchlorate) and DiD (1,1'-dioctadecyl-3,3,3', 3'-tetramethylindodicarbocyanine, 4-chlorobenzenesulfonate ) (Invitrogen)), with one tracer injected deep into the paw and the second injected as was DiI. Following harvest of dorsal root ganglia (DRG) for recording, rats were perfused with saline followed by 4% paraformaldehyde (Sigma-Aldrich). The hindpaw was harvested, post-fixed for an hour and then cryoprotected in 30% sucrose overnight. The site of dye injection was harvested in ~1$cm^2$ block to a depth of the underlying bones. Tissue was cut on either a cryostat (16 μm) or a freezing microtome (30 μm).

### 2.3. Tissue inflammation

Two to three weeks after labeling, inflammation was induced at the site of DiI injection in the left hindpaw with a subcutaneous injection of complete Freund's adjuvant (CFA, Sigma-Aldrich). CFA was diluted 1:1 in 0.9% sterile saline and injected (100 μl) with a 25 g needle under isoflurane anaesthesia. DRG were harvested for study 3 days after CFA injection. This time point was chosen for 3 main reasons: 1) the time point corresponds to the peak hyperalgesia [40], 2) 3 days is long enough for the development of changes in transcription/translation of proteins that are involved in the sensory neuron response to inflammation [40], and 3) longer time points were not used in order to minimize the duration animals are forced to live with persistent inflammation.

### 2.4. Cell dissociation

Rats were deeply anaesthetized with a subcutaneous injection (1 ml/kg) of rat cocktail (consisting of 55 mg/ml ketamine, 5.5 mg/ml xylazine, and 1.1 mg/ml acepromazine) (ketamine was from Fort Dodge Animal Health, Fort Dodge, WI, USA; xylazine and acepromazine were from Phoenix Scientific Inc., St Joseph, MO, USA). $L_{4\text{-}5}$ DRG were harvested bilaterally, but processed independently in order to study neurons ipsilateral and contralateral to the site of inflammation. Harvested ganglia were enzymatically treated, mechanically dissociated and plated on laminin and ornithine coated cover-slips as previously described [36]. All experiments were performed within 8 h of tissue harvest.

### 2.5. Classification of cutaneous DRG neurons

Cutaneous DRG neurons were classified on the basis of a combination of three criteria: DiI labeling, cell body size and responsiveness to the algogenic compound capsaicin (CAP, Sigma-Aldrich). DiI was used to identify neurons innervating the site of inflammation as both DiI and CFA were injected into the same site. Neurons were divided into small (30 μm), medium (30–40 μm), and large (·40 μm) based on cell body diameter which was measured with a calibrated eyepiece reticule. Neurons in which application of CAP (500 nM) resulted in an inward current > 50 pA (~2 × the size of spontaneous fluctuations) from a holding potential of −60 mV were considered CAP responsive. CAP was applied at the end of each experiment. Only 1 neuron was studied per coverslip.

While additional criteria including magnitude and kinetics of responses to ATP, α, β-methyl-ATP and protons, properties of the action potential waveform and magnitude of currents such as $I_h$ and $I_A$ have been employed to define additional subpopulations of sensory neurons *in vitro* [13,45] and results from these studies suggest it is possible to identify several subpopulations of putative nociceptive neurons *in vitro*, we chose to restrict our criteria for subclassification of cutaneous DRG neurons to cell body size and capsaicin sensitivity for 3 main reasons. First, despite recent evidence that cell body size may have limited utility for the identification of some subpopulations of putative nociceptors [25,21], cutaneous DRG neurons constitute the subpopulation for which there is the most compelling justification for the use of this criterion [32,18]. Second, the combination of cell body size and capsaicin sensitivity is easy to employ enabling identification of a large proportion of putative nociceptive afferents. Third, these two criteria have been widely used by other investigators [47,48,44,14,5,10,39], enabling comparisons between data sets.

### 2.6. Electrophysiological recording

Whole-cell patch-clamp recordings were performed using an EPC-9 amplifier (HEKA Elektronik GmbH, Lambrecht, Germany). Series resistance was compensated (80%) with amplifier circuitry. Data were acquired at 10 kHz and filtered at 2 kHz. Electrodes (1.8–3.0MΩ) were filled with pipette solution (mM): 100 Cs-Methansulphonate (MS), 5 Na-MS, 40 TEA-Cl, 1 $CaCl_2$, 2 $MgCl_2$, 11 EGTA, 10 HEPES, 2 ATP-Mg, 1 GTP-Li); pH was adjusted to 7.2 with Tris-base and osmolality was adjusted to 310 mosmol/l with sucrose. The bath solution was constructed to minimize other cation currents in sensory neurons and contained (mM): 100 Choline-Cl, 30 TEA-Cl, 2.5 $CaCl_2$, 0.6 $MgCl_2$, 10 HEPES, 10 Glucose; pH was adjusted to 7.4 with Tris-base and osmolality was adjusted to 325 mosmol/l with sucrose. All salts were obtained from Sigma-Aldrich (St. Louis, MO). Sucrose was obtained from Thermo-Fisher (Pittsburgh, PA).

Neurons were held at 60 mV. Currents were evoked with a series of 60 ms voltage steps from ·80 to 65 mV in 5 mV increments following a 100 ms prepulse to 100 mV. Leak currents were digitally subtracted using a P/−4 leak subtraction protocol from a holding potential of 80 mV. A neuron was considered to have low threshold (LVA) current if the peak inward current evoked at −30 mV was 2 standard deviations greater than the mean peak inward current fluctuation measured in response to voltage steps to −65, −60 and −55 mV. Peak high threshold (HVA) current was measured at 0 mV. $Ca^{2+}$ current density was determined by dividing peak current by cell capacitance. Conductance-voltage (G-V) curves for $Ca^{2+}$ currents were derived from instantaneous I-V data obtained from tail currents at −60 mV. Parameters of $Ca^{2+}$ current activation were derived from G-V data fitted with a Boltzmann equation of the form: $G$ = fitted maximal $G_{max}/(1+\exp[(V_m - V_{1/2})/k])$, where $G$ = observed conductance, $G_{max}$ = the conductance, or availability, $V_{1/2}$ = the potential for half activation $V_m$ = command potential and $k$ = the slope factor. G-V data from neurons with LVA currents were fitted with a double Boltzmann equation of the form: $G = G_{max}1/(1+\exp((V_m - V_{1/2}1)/k1))+G_{max}2/(1+\exp((V_m - V_{1/2}2)/k2))$, where "1" and "2" are parameters for LVA and HVA currents, respectively. Steady-state inactivation was assessed with 1 second voltage-steps to potentials ranging from −100 mV to +10 mV followed by a voltage step to 0 mV. Current availability data (peak evoked current at the test potential vs pre-pulse potential) were fitted with single Boltzmann equation which was modified to enable estimation of the fraction of non-inactivatable current as previously described [23].

To assess the relative density of HVA current subtypes among cutaneous DRG neurons as well as the impact of inflammation on the relative current density, nifedipine (10 μM, Sigma-Aldrich), ω-conotoxin GVIA (CTx, 200 nM, Alomone Labs, Jerusalem Isreal) and ω-agatoxin IVA (AgTx, 200 nM, Alomone Labs) were used to isolate L-, N- and P/Q-type currents,

respectively. Pilot studies were conducted to confirm that the concentration of each blocker used was saturating (i.e., 400 nM CTX produced no additional block than 200 nM CTX, data not shown).

Current clamp experiments were performed on small and medium diameter cutaneous DRG neurons using the EPC-9 amplifier in fast-current clamp mode. Data were acquired at 10 kHz and filtered at 2 kHz. Electrodes (1.8–3.0Mω) were filled with pipette solution (mM): 140 K-methansulfonate, 5 NaCl, 1 $CaCl_2$, 2 $MgCl_2$, 11 EGTA, 10 HEPES, 2 ATP-Mg, 1 GTP-Li; pH was adjusted to 7.2 with Tris-base and osmolality was adjusted to 310 mosmol/l with sucrose. The recording chamber was continuously perfused with a physiological bath solution containing (mM): 140 NaCl, 3 KCl, 2.5 $CaCl_2$, 0.6 $MgCl_2$, 10 HEPES, 10 Glucose; pH was adjusted to 7.4 with Tris-base and osmolality was adjusted to 325 mosmol/l with sucrose. Passive and active electrophysiological data were obtained before and after application of 5 μM $CdCl_2$, to partially block VGCC. Resting membrane potential was continuously monitored. An action potential was evoked with a 4 ms current injection from rest as well as from −60 mV, a potential obtained with DC current injection. Properties of the action potential (AP) waveform that were analyzed included: 1) maximum rate of AP rise and fall (determined from the first derivative of the action potential waveform); 2) AP over-shoot (above 0 mV), 3) duration (at 0 mV), 4) afterhyperpolarization (AHP) magnitude (relative to resting membrane potential); 5) AHP decay (determined with a single exponential).

At least 3 minutes of baseline excitability data were collected for each neuron prior to the bath application of $Cd^{2+}$ (5 μM). This concentration of $Cd^{2+}$ was chosen based on results from preliminary experiments indicating that 5 μM $Cd^{2+}$ blocked 41.1 ± 0.07% (n = 10) of the HVA current evoked at 0 mV. Baseline excitability was assessed in 1 of two ways: With “square-wave” or “ramp and hold” stimuli. The square-wave stimuli consisted of a 750 ms current injection where AP threshold was defined as the maximum depolarization obtained in the absence of an AP and rheobase was defined the minimum depolarizing current injection necessary to evoke an AP [24]. The total number of APs evoked in response to suprathreshold stimuli was assessed by stimulating neurons with depolarizing current injection equal to 2 and 3 times rheobase. The size of the current injection increment used to determine AP threshold and rheobase was scaled as a function of rheobase such that increments of 5 or 10 pA were used depending on whether rheobase was <50 or >50 pA, respectively). This set of stimuli was applied once per minute over a period of at least three minutes, in order to establish baseline excitability.

The ramp and hold stimulus consisted of a 250 ms ramp to an amplitude that was held for an additional 500 ms. The amplitude of the stimulus was adjusted so that an AP was evoked towards the end of the ramp. Because the latency to the AP is a measure of both the AP and current threshold (current necessary to evoke an AP), and subsequent APs are a measure of accommodation [22], a single protocol could be used to assess several aspects of excitability. After establishing the baseline AP and current threshold, and the response to suprathreshold stimuli with “square-wave” stimuli, the ramp and hold stimulus was used to monitor stability prior to the application of $Cd^{2+}$ with at least 90 seconds of data collected at an inter-stimulus-interval (ISI) of 30 sec. The effects of $Cd^{2+}$ were only assessed in neurons demonstrating stable baseline excitability. Results obtained with both square-wave and ramp and hold stimuli were comparable. A neuron was considered responsive to $Cd^{2+}$, if there was a change in any parameter of excitability (AP threshold, current threshold or accommodation) > 2 standard deviations from the baseline mean. The effects of $Cd^{2+}$ were analyzed relative to baseline data.

### 2.7. Semi-quantitative RT-PCR (sqRT-PCR)

Dorsal root ganglia (DRG) from anesthetized male rats were harvested in a manner identical to that used for neuron isolation and plating. Trizol reagent (Invitrogen) was used to extract

RNA according to the manufacturer's protocol. First-strand cDNA synthesis was carried out using 1μg total RNA with SuperScript II reverse transcriptase and an anchored oligo $(dT)_{12–18}$ primer. SYBR Green was used to monitor amplification of template with primers on a real-time thermal cycler (Applied Biosciences) controlled by a PC running Prism 7000 SDS software. A melting curve was generated at the end of each experiment to assess for the presence of contamination. Amplification efficiency was determined for each target gene. The ΔΔCT method is used to assess differences in relative expression levels following confirmation that inflammation has no effect on comparator gene (e.g., GAPDH). Primers for amplification of α2δ1 (accession # M86621) $Ca^{2+}$ channel subunit complex were: F – TGAGTTGTTTCCAGCACCTG, R – CTCTTCTCCTCCATCCGTGA; those for amplification of $Ca_V2.2$ (accession # NM 147141.1) were: F – AAGGCGCTGCCCTACGT, R- GCCGATGATGGCGTAGATG; while those for GAPDH (accession # XR 008198) were: F – GGCCTACATGGCCTCCAA, R – TGGAATTGTGAGGGAGATGCT.

### 2.8. Western Blot

L4 and L5 DRG, the nerve central to the DRG (~1 cm)was rapidly removed from deeply anesthetized rats and homogenized in solubilization buffer (50 mM Tris.HCl, pH8.0; 150 mM NaCl, 1 mM EDTA, 1% NP40, 0.5% deoxycholic acid, 0.1% SDS, 1 mM $Na_3VO4$, 1 U/ml aprotinin, 20 μg/ml leupetin, 20 μg/ml pepstatin A). The homogenate was centrifuged at 20,200 X g for 10 min at 4°C. The supernatant was removed. Protein (50–120 μg) was separated on a 7.5–10% SDS-PAGE gel and blotted to nitrocellulose membrane (Amersham) with a Trans-Blot Transfer Cell system (Bio-Rad). Blots were blocked with 5% milk in TBS buffer (20 mM Tris, 150 mM NaCl pH 7.4) at room temp for 30 min. After decanting the blocking buffer, the blot is incubated with the respective antibody. These included: α2δ1 (AKA Cacna2d1, Ab D219, Sigma: 1:200), $Ca_V2.2$ (AKA Cacna1b, α1b, Ab51, 1:500, Generous gift from Dr. Elise Stanley), and GAPDH (sc-25778, Santa Cruz Biotechnology: 1:1000). Membranes were incubated with α2δ1 and $Ca_V2.2$ antibodies overnight at 4°C, and GAPDH for 1 h at room temperature. Membranes were washed with TBS buffer and incubated for 1 hour with anti-goat IgG horseradish peroxidase (1:3000, Santa Cruz) in 5% milk/TBS. Membranes were then washed with TBS buffer. The immunoreactivity was detected using Enhanced Chemiluminescence (ECL, Amersham). Chemiluminescence was captured with a CCD camera (Las-3000, Fujifilm) and analyzed with Fuji software Multi Gauge. The relative protein levels were obtained by comparing target protein to loading control (GAPDH) in the same membrane.

### 2.9. Statistical analysis

Data are expressed as mean ± S.E.M unless otherwise stated. Student's t test, one- and two-way ANOVA with the Holm-Sidak post hoc test were used for comparisons of parametric data between groups. A paired t-test was used to assess the impact of $Cd^{2+}$ on passive and active electrophysiological properties. Chi-square or Fisher Exact tests were used for comparisons of non-parametric data between groups. Statistical significant was assessed at $p<0.05$.

## 3. Results

### 3.1. Retrograde labeling

Analysis of the distribution of tracer in the hindpaw indicated that in each animal studied (n = 5), DiI was restricted to the dermis, a layer corresponding to the location of the plexus of fibers giving rise to cutaneous innervation [33]. Double label experiments indicated that while there was some spread of the "deep" injection into a zone labeled by the more superficial injection, there was no detectable spread of tracer in the other direction (Supplementary Figure 1). These observations suggest that the spread of DiI in cutaneous tissue is minimal. Therefore, while it is possible that neurons innervating superficial structures such as blood vessels and muscle

were labeled with DiI, the majority of retrogradely labeled neurons studied were likely cutaneous afferents.

Cutaneous DRG neurons from 6 naïve and 12 inflamed rats were studied with patch clamp electrophysiological techniques. From these, 85 neurons were from naïve and 173 were from inflamed rats. 113 and 60 neurons from inflamed rats were from DRG ipsilateral and contralateral to the site of inflammation, respectively. Neurons were further sub-classified according to cell body diameter and capsaicin sensitivity. Data from neurons from naïve rats were first compared with those from cutaneous neurons contralateral to the site of inflammation. No statistically significant differences were detected between these groups of neurons with respect to any of the parameters analyzed (i.e., cell body diameter, capsaicin sensitivity, $Ca^{2+}$ current density, etc.). Therefore, data from these two groups of neurons were pooled and referred to as control neurons in subsequent analyses.

### 3.2. $Ca^{2+}$ currents in subpopulations of cutaneous DRG neurons

While $Ca^{2+}$ currents studied with the standard whole-cell configuration of patch clamp may be subject to relatively large time dependent changes (i.e., run-up or run-down), currents in the present study were relatively stable. In a series of control experiments in which current was evoked every 15 seconds for the first 3 minutes following establishment of whole cell access, time-dependent changes in peak current were small: the average change was a 3.5 ± 2.2% decrease over this period (n = 28) in neurons from naïve rats and a 4.2 ± 3.9% (n = 33) increase in neurons from inflamed rats. These values were not significantly different ($p > 0.05$, Student's t test). Nevertheless, to control for the influence of time-dependent changes in currents evoked from cutaneous DRG neurons, the I-V protocol (see methods and Figure 1A) used to evoke currents was initiated 3 minutes after establishing whole cell access in all neurons studied.

HVA currents (Figure 1) were present in every neuron studied. These currents had a threshold for activation between −25 and −20 mV with peak inward current evoked at between 0 and 5 mV. While relatively large (i.e., >500 pA at −30 mV) LVA currents have been described in a subpopulation of sensory neurons [47], only a small (i.e., less than 400 pA at −30 mV, mean −161.8 ± 12.1 pA) LVA current was detected in 49.6% (61/123) of control cutaneous DRG neurons. In marked contrast to HVA currents which did not begin to activate at potentials < −25 mV, LVA current was detectable at ~−45mV.

Consistent with previous results from our laboratory [36] as well as those of others [47], there were significant differences between subpopulations of neurons defined by cell body size with respect to the magnitude and biophysical properties of HVA current. HVA current was largest in the large and smallest in the small diameter neurons: peak current at 0 mV was 8.27 ± 1.01 nA (n = 12), 4.62 ± 0.36 nA (n = 24) and 3.20 ± 0.29 nA, (n = 32) in large, medium and small diameter neurons, respectively ($p < 0.01$, one-way ANOVA). Differences in current magnitude were not entirely a reflection of cell body size, as current normalized to membrane capacitance was still significantly larger in large diameter than in small diameter neurons (Figure 1B; $p<0.01$, one-way ANOVA). There were also small, but significant differences between subpopulations of neurons defined by cell body diameter with respect to the voltage-dependence of current activation (Figure 1C and Table 1). There were no statistically significant ($p > 0.05$, Students t-test) differences between subpopulations of neurons defined by capsaicin sensitivity with respect to peak HVA current (which was 3.76 ± 0.41 nA, (n = 24) and 4.76 ± 0.56 nA, (n = 36) in capsaicin responsive (CAP+) and unresponsive (CAP-) neurons, respectively) current density or the voltage dependence of activation (Table 1).

### 3.3. Impact of inflammation on cutaneous DRG neurons

CFA was injected into the same site as the DiI+ injection 3 days prior to recording. Cutaneous DRG neurons were studied in the order that they were detected under epifluorescence illumination. Following dissociation, this approach should have yielded a "random" sampling of neurons enabling the assessment of the impact of inflammation on cell body diameter. The median cell body diameter was 30.0 (with 28.2 and 33.1 as $25^{th}$ and $75^{th}$ percentiles, respectively), 30.0 (27.5 and 38.0) and 31.3 μm (29.0 and 34.3) for naïve neurons and neurons from DRG contralateral and ipsilateral to the site of CFA injection, respectively. There was no statistically significant difference between groups ($p > 0.05$, one-way ANOVA). Similar results were obtained when cell body capacitance, a measure of membrane surface area, was used as a measure of cell body size (Figure 2A). While there was no statistically significant influence of CFA on the proportion of CAP+ neurons (26 of 63 control neurons versus 22 of 46 inflamed neurons, $p > 0.05$, Chi-square test), the CAP evoked response in neurons ipsilateral to the site of inflammation was significantly larger than that in control neurons (i.e., naïve rats and from neurons contralateral to the site of inflammation) (Figure 2B and C, $p < 0.05$, Student t-test). Consistent with the suggestion that the increase in CAP current was associated with an increase in TRPV1 channel activity in neurons in which this channel was already present, there was no detectable influence of inflammation on cell body size of CAP+ neurons which was 42 ± 3.0 and 47 ± 3.3 ($p > 0.05$, Student's t-test) in neurons from control and inflamed rats, respectively.

### 3.4. Impact of inflammation on $Ca^{2+}$ currents in cutaneous DRG neurons

Comparing HVA current density data from control neurons to that from inflamed neurons with two-way ANOVA revealed significant main effects associated with both size ($p < 0.01$) and inflammation ($p < 0.01$) (Figure 3A, B and C). There was, however, no significant interaction between these two factors. When data were analyzed as a percent of the mean peak current density in control neurons, the current decrease in neurons from CFA treated rats was significantly ($p < 0.01$, one-way ANOVA) larger in small (42.3 ± 7%) and medium (24.0 ± 5.4%) diameter neurons than that in large (3.7 ± 15.9%) diameter neurons. The difference between small and medium diameter neurons was not statistically significant ($p > 0.05$). The inflammation-induced decrease in current density was not associated with a detectable change in the voltage-dependence of current activation, as illustrated by virtually overlapping G-V curves (Figure 3D, E and F). Parameters describing the voltage-dependence of HVA current activation in subpopulations of cutaneous from control and inflamed rats are summarized in Table 1.

A similar analysis was performed on data from subpopulations of cutaneous DRG neurons defined by capsaicin sensitivity (Figure 4 and Table 1). Two-way ANOVA revealed a significant main effect associated with inflammation ($p < 0.01$) but the main effect of CAP sensitivity was not statistically significant ($p > 0.05$), nor was there an interaction between these two factors ($p > 0.05$).

While the 100 ms pre-pulse to -100 mV should have mitigated the impact of a shift in steady-state inactivation on the availability of HVA currents in cutaneous DRG neurons, steady-state inactivation was assessed in 9 small diameter cutaneous neurons from 2 inflamed rats to directly assess this possibility. A 1 second pre-pulse was used to drive channel inactivation. Results from this analysis suggested that HVA current in cutaneous neurons was fully available for activation at a holding potential of −60 mV given that the midpoint of steady-state inactivation was −16 ± 4 mV with a slope factor of 15 ± 1.5. The fraction of current resistant to steady-state inactivation in these neurons was 0.47 ± 0.04. These results confirm that the inflammation induced decrease in current density was not due to an increase in the inactivation of HVA current in cutaneous DRG neurons.

### 3.5. Impact of inflammation on subtypes of HVA currents in cutaneous DRG neurons

To determine which types of $Ca^{2+}$ channel were reduced by the presence of persistent inflammation, we assessed the relative density of L-, N- and P/Q-type currents in small and medium diameter cutaneous DRG neurons from naïve and inflamed rats. L-, N- and P/Q-type currents were isolated as described in Methods with nifedipine (10 μM), ω-conotoxin GVIA (CTx, 200 nM) and ω-agatoxin IVA (AgTx, 200 nM), respectively. Blockers were added to each neuron in a sequential manner as illustrated in Figure 5(A and B). $Cd^{2+}$ (50 μM) was used to confirm that current remaining in the presence of the combination of blockers was residual voltage-gated $Ca^{2+}$ current (likely carried by R-type channels [15]). The order of application was varied from cell to cell to mitigate time-dependent influences on estimates of relative current density. There was no statistically significant difference between small and medium diameter neurons from naïve rats with respect to the distribution of L, N, and P/Q type currents as a fraction of the total current in each neuron ($p > 0.05$, Chi-Square test; Table 2). There was also no statistically significant influence of inflammation on this distribution ($p > 0.05$, Students t and chi-square tests; Table 2). The absence of a detectable shift in the relative distribution of current types suggested that the inflammation-induced decrease in HVA current was not subtype specific. Consistent with this suggestion, analysis of the percent change in the density of each HVA current subtype revealed that all subtypes were reduced in small diameter neurons from inflamed rats (Fig. 5C), including residual current insensitive to nifedipine, CTx and AgTx. There was no statistically significant ($p > 0.05$, one-way ANOVA) difference between subtypes with respect to the magnitude of the percent decrease in current density. Similar results were obtained for medium diameter neurons (Fig. 5D), except that there was an increase in the density of residual current.

### 3.6. Impact of inflammation on $Ca^{2+}$ currents in unlabeled DRG neurons

To determine whether the impact of persistent inflammation on current density was restricted to neurons innervating the site of inflammation, we assess the impact of inflammation on current density in unlabeled neurons. There was no statistically significant difference between unlabeled control neurons and unlabeled neurons ipsilateral to the site of CFA injection with respect to HVA current magnitude, conductance density or the voltage-dependence of activation, whether neurons were classified according to cell body diameter or capsaicin sensitivity. For example, peak current in small, medium and large diameter unlabeled neurons from ganglia ipsilateral to the site of inflammation was 2.66 ± 0.43 nA (n = 6), 6.97 ± 1.83 nA (n = 13) and 11.94 ± 2.98 nA (n = 9), respectively. These values are not significantly different from those from the same subpopulations of control neurons (3.01 ± 0.41 (n=17), 4.33 ± 0.39 (n=21) and 19.17 ± 3.05 (n=12) nA in small, medium and large diameter neurons respectively). A relatively large (>500 pA at −30 mV) LVA current was detected in a subpopulation (8/21) of unlabeled medium diameter control neurons, and this proportion was significantly reduced ($p = 0.01$, Fisher exact test) to 0/13 in unlabeled neurons from ganglia ipsilateral to the site of inflammation. There was no statistically significant change in either proportion of unlabeled neurons with a small LVA current (11/28, 39.3%) from inflamed rats or the magnitude of the small LVA current in these neurons (−230.6 ± 42.6 pA, n = 11).

### 3.7. Excitability of cutaneous DRG neurons following inhibition of $Ca^{2+}$ currents

To begin to assess the functional consequences of the inflammation-induced decrease in HVA current in cutaneous afferents, small and diameter cutaneous DRG neurons from naïve rats were studied in current clamp. Excitability, as assessed with depolarizing current injection, was assessed before and after application of 5 μM $Cd^{2+}$, which was used to block ~40% of the HVA current. This degree of fractional block was chosen to mimic the extent of current reduction associated with the presence of inflammation. A change in any measure of excitability (action potential (AP) threshold, current threshold or the number of spikes evoked

during sustained current injection) was considered a response to $Cd^{2+}$. Sixty-five percent (15 of 23) of the neurons tested responded to $Cd^{2+}$ with a change in excitability. Of these, an increase in excitability was observed in 7 neurons and a decrease in excitability was observed in 8 neurons (Figure 6). The increase in excitability was associated with a small but significant decrease in current threshold and an increase in the response to suprathreshold stimuli (Fig 6). Reversibility of the $Cd^{2+}$-induced changes in excitability was assessed in 3 of the neurons in which excitability was decreased and 4 of the neurons in which excitability was increased; changes in excitability reversed on all 7 neurons (data not shown). These changes in excitability were associated with an increase in AP overshoot ($p = 0.01$), duration ($p < 0.01$), and rates or rise ($p = 0.01$) and fall ($p < 0.01$) (Table 3). The decrease in excitability was generally associated with a decrease in the response to suprathreshold stimuli. These changes in excitability were not associated with consistent, and therefore statistically significant, changes in AP waveform (Table 3). There were no obvious differences between neurons in which excitability was increased, decreased or unchanged by the application of $Cd^{2+}$.

### 3.8. Inflammation increases α2δ1 subunit expression in DRG

To begin to assess the basis for the inflammation-induced decrease in HVA current in cutaneous DRG neurons, we sought to determine whether inflammation was associated with a change in the expression of $Ca^{2+}$ channel subunits. We started by assessing changes in $Ca_V2.2$, the α subunit responsible for N-type currents [15], since this was the dominant current in cutaneous DRG neurons and was significantly reduced in the presence of inflammation. Sq-RT-PCR analysis of mRNA extracted from L4 and L5 DRG harvested from naïve ($n = 8$) and inflamed ($n = 7$) rats reveled no detectable change in $Ca_V2.2$ mRNA levels and no difference between mRNA levels in DRG ispilateral ($n = 7$) or contralateral ($n = 4$) to the site of inflammation (Figure 7A). Because the α2δ subunit plays a role in trafficking all $Ca^{2+}$ channel α subunits to the cell membrane [17] and out of the sensory neuron cell body [6], and the α2δ1 subunit complex is present in primary afferents [50], we next assessed the impact of inflammation on α2δ1 subunit mRNA. In contrast to $Ca_V2.2$ expression, and to our expectations, we detected a significant ($p < 0.01$) increase in α2δ1-subunit mRNA in DRG ispilateral to the site of inflammation (Figure 7B). Because an increase in α2δ1 protein might have been expected to increase in current density [34], the combination of our electrophysiological and sqRT-PCR data raised the possibility that the decrease in current density at the cell body was due to an increase in channel trafficking out of the ganglia.

### 3.9. Inflammation increases $Ca^{2+}$ channel subunit density in sensory axons

To test the possibility that the inflammation-induced increase in α2δ1 subunit mRNA results in an increase in $Ca^{2+}$ channel trafficking out of the ganglia, we assessed subunit protein levels in the central nerves (i.e,. the nerve between the DRG and the spinal cord) from L4 and L5 DRG from inflamed (ipsilateral and contralateral) and naïve rats (Fig. 8). Protein was quantified with Western blot. Results of this analysis revealed an increase ($p = 0.02$, one way ANOVA) in both $Ca_V2.2$ and α2δ1 levels in central nerves ipsilateral to the site of inflammation compared to that in the contralateral nerves or in nerves from naïve rats.

## 4. Discussion

We have described the impact of inflammation on voltage-gated $Ca^{2+}$ currents in cutaneous DRG neurons. The most striking observations in this study were: 1) an inflammation-induced reduction in HVA currents in small and medium, but not large diameter cutaneous DRG neurons; 2) the decrease was restricted to neurons innervating the site of inflammation; 3) the decrease was associated with a reduction of all pharmacologically defined types of HVA current; 4) a reduction in HVA current comparable to that associated with inflammation differentially influenced the excitability of subpopulations of cutaneous DRG neurons with an

increase in excitability in one and a decrease in excitability in another; 5) an inflammation-induced increase in α2δ1-subunit, but no change in $Ca_V2.2$, mRNA; and 6) an inflammation-induced increase in α2δ1 and $Ca_V2.2$ protein in the central nerves of L4 and L5 ganglia ipsilateral to the site of inflammation.

Based on the criteria used to identify putative nociceptors in the present study, our results suggest that inflammation-induced decreases in HVA current are largely restricted to putative nociceptive neurons. It is also likely, however, that smaller but significant inflammation-induced decreases in HVA current also occurred in subpopulations of non-nociceptive neurons as demonstrated by the decrease in HVA current in medium diameter CAP– neurons and the decrease in LT-VGCC in medium diameter CAP– and unlabeled neurons. The latter observation is the most compelling in this regard, given evidence that large LVA currents are present in D-hair afferents [19].

The distribution of $Ca^{2+}$ currents among subpopulations of unlabeled neurons defined by cell body diameter and/or capsaicin sensitivity observed in the present study is consistent with results from previous studies [47,36]. This is true for both HVA currents, which were present in the highest density in large diameter DRG neurons, and LVA currents which were present in the form of uniquely large currents in a subpopulation of medium diameter neurons [47, 36]. While a subpopulation of small diameter DRG neurons with large LVA currents has been described [42], we did not encounter such neurons in the present study. Our failure to detect such a population may reflect the fact that the voltage-clamp protocol used to evoke $Ca^{2+}$ currents was not optimized for the characterization of LVA current, although we were clearly able to detect such currents in medium diameter neurons.

The relative density of L- and N-type currents in cutaneous DRG neurons is similar to that previously reported in a subpopulation of putative nociceptive neurons, referred to as “type 2” neurons, where L- and N-type currents constituted 23% and 42% of the total current, respectively [13]. “Type 2” neurons had a small cell body diameter, a relatively short action potential duration, had negligible $I_H$ currents, but a relatively large $I_A$ current and were responsive to capsaicin. Additional support for the suggestion that “Type 2” neurons were nociceptors came from the observation that the inflammatory mediator, serotonin, selectively increased tetrodotoxin (TTX) resistant voltage-gated $Na^+$ currents in this subpopulation of DRG neurons [12]. Together, these previous observations provide additional support for the suggestion that inflammation-induced changes in $Ca^{2+}$ currents are primarily manifest in cutaneous nociceptors.

There were both similarities and differences between our observations of the impact of inflammation on cutaneous DRG neurons and those of previous investigators. While we [21] and others [41] have reported inflammation-induced increases in the membrane capacitance and/or cell body size in specific subpopulations of sensory neurons, we detected changes in neither of these properties in the present study. This observation suggests that this particular response to inflammation may be tissue specific with changes in joint [21] or visceral [41] but not cutaneous afferents. A tissue specific response to inflammation may also account for our failure to detect a significant increase in the proportion of capsaicin responsive neurons as has been reported by others [30,2,10] given that retrograde tracers were not used in these previous studies. However, the increase in the magnitude of evoked current observed in the present study is consistent with inflammation-induced increases in TRPV1 protein [30] and current magnitude [10] observed by others.

The inflammation-induced decrease in HVA current observed in the present study was in the opposite direction to what we had predicted. Nevertheless, we suggest the decrease in HVA current observed is a specific response to inflammation rather than a non-specific effect such

as an over-all decrease in the health of the neurons because the decrease was observed in specific subpopulations of neurons in the face of increases in capsaicin evoked current. While we did not assess expression levels of all HVA-channel subtypes, and a decrease in mRNA expression in a subpopulation of neurons may not have been detected at a whole ganglion level, the fact that we were unable to detect a change in $Ca_V2.2$ mRNA suggests that a decrease in channel expression is unlikely to be the primary mechanism underlying the inflammation-induced decrease in current density. Similarly, the absence of a detectable change in the voltage-dependence of channel activation or an increase in steady-state inactivation, argues against a post-translational change in channel gating.

We suggest an alternative explanation for the decrease in current density in light of the *increase* in α2δ1 mRNA in combination with the increase in channel protein in the central nerves of L4 and L5 ganglia ispilateral to the site of inflammation: that there is an increase in the $Ca^{2+}$ channel trafficking out of the cell body. Minimally, the fact that there was no detectable change in current density in unlabeled neurons suggests the changes in subunit expression and protein distribution reflect changes in a subpopulation of cutaneous DRG neurons. More importantly, our results suggest that inflammation is associated with a redistribution of $Ca^{2+}$ channels in primary afferents. An increase in current density at central and/or peripheral terminals would contribute to an increase in transmitter release and consequently the pain and/or neurogenic component of an ongoing inflammatory response. Conversely, as suggested by our current clamp data, decreases in current density, at sites where channels are trafficked away from, may result in changes in excitability (see below). Given the more dramatic increase in α2δ1 expression in primary afferents following nerve injury [37] in combination with reported decreases in $Ca^{2+}$ currents in DRG neurons following nerve injury [4,27,1,38,39], a redistribution of $Ca^{2+}$ channels may be a response common to inflammation and peripheral neuropathy [6].

Variability in the observed impact of a decrease in HVA current on the excitability of cutaneous DRG neurons is consistent with previous data indicating that the excitability of these neurons is largely determined by other ion channels [9]. Nevertheless, the observation that a decrease in $Ca^{2+}$ current resulted in a decrease in excitability in a subpopulation of neurons, suggests that in at least some neurons, HVA currents contribute to AP generation. Furthermore, in a subpopulation of neurons in which partial block of HVA currents resulted in a decrease in excitability, a decrease in the AP duration was also observed (data not shown). Interestingly, however, while both changes should result in a decrease in $Ca^{2+}$ influx, and therefore a decrease in magnitude and/or increase in the decay of evoked $Ca^{2+}$ transients, we recently reported that $Ca^{2+}$ transients are increased by inflammation in cutaneous neurons [35]. Taken together, these observations indicate that inflammation is associated with the differential regulation of at least two processes controlling the magnitude and decay of $Ca^{2+}$ transients in cutaneous neurons.

In all neurons in which partial block of HVA currents resulted in an increase in excitability, an increase in the AP duration was also observed. This change is consistent with the suggestion that $Ca^{2+}$ influx via HVA channels is coupled to $Ca^{2+}$-dependent $K^+$ channels [7] which contribute to the regulation of both excitability and AP duration in a subpopulation of sensory neurons [46,51]. Consistent with the suggestion that a decrease in $Ca^{2+}$ current contributes to an inflammation-induced increase in the excitability of at least a subpopulation of cutaneous afferents, we have reported that persistent inflammation increases the excitability of cutaneous afferents [31]. Importantly, both changes should result in an increase in $Ca^{2+}$ transients and a distinct pattern of changes in $Ca^{2+}$ signaling than in those afferents in which a decrease in HVA current was associated with a decrease in excitability. Taken together, these results suggest that the inflammation-induced decrease in $Ca^{2+}$ current will have both a qualitative and a quantitative impact on afferent properties.

Ultimately, the physiological impact of an inflammation-induced change in HVA current in cutaneous afferent will depend on the context in which these changes are manifest *in vivo*. If inflammation-induced changes in channel trafficking result in an increase in current density at the terminals, such a change should facilitate $Ca^{2+}$ influx and subsequent transmitter release if channels are clustered at release sites (although this is not always the case [11]). Decreases in current density at the cell body may also be critical for limiting $Ca^{2+}$-induced excitotoxicity that could result from ongoing activity in a subpopulation of afferents that are normally inactive, as well as sculpting the magnitude and decay of evoked $Ca^{2+}$ transients critical for activity-dependent changes in gene expression [20] and/or transmitter release. Alternatively, a decrease in HVA channels coupled to $Ca^{2+}$-dependent $K^+$ currents [7] would result in an increase in afferent excitability that could contribute to the ongoing pain and/or hypersensitivity of persistent inflammation.

## Supplementary Material

Refer to Web version on PubMed Central for supplementary material.

## Acknowledgments

We would like to thank Dr. Gerald Gebhart and Andrea Vaughn for helpful comments in the preparation of this manuscript. We would like to thank Dr. Elise Stanley for the generous gift of the CaV2.2 antibody. And we would like to thank Dr. Liming Fan and Marcel Charbonnet for technical assistance. This work was supported by NIH grant NS 44992 (MSG) DE018252 (MSG). None of the authors of this manuscript have a conflict of interest with any of the work described in this manuscript.

## References

1. Abdulla FA, Smith PA. Axotomy- and autotomy-induced changes in Ca2+ and K+ channel currents of rat dorsal root ganglion neurons. J Neurophysiol 2001;85:644–658. [PubMed: 11160500]
2. Amaya F, Shimosato G, Nagano M, Ueda M, Hashimoto S, Tanaka Y, Suzuki H, Tanaka M. NGF and GDNF differentially regulate TRPV1 expression that contributes to development of inflammatory thermal hyperalgesia. Eur J Neurosci 2004;20:2303–2310. [PubMed: 15525272]
3. Amir R, Argoff CE, Bennett GJ, Cummins TR, Durieux ME, Gerner P, Gold MS, Porreca F, Strichartz GR. The role of sodium channels in chronic inflammatory and neuropathic pain. J Pain 2006;7:S1–29. [PubMed: 16632328]
4. Baccei ML, Kocsis JD. Effect of axotomy on voltage-gated barium currents in adult rat cutaneous afferent neurons. Soc Neurosci Abs 1999;25:408.
5. Baccei ML, Kocsis JD. Voltage-gated calcium currents in axotomized adult rat cutaneous afferent neurons. J Neurophysiol 2000;83:2227–2238. [PubMed: 10758131]
6. Bauer CS, Nieto-Rostro M, Rahman W, Tran-Van-Minh A, Ferron L, Douglas L, Kadurin I, Sri Ranjan Y, Fernandez-Alacid L, Millar NS, Dickenson AH, Lujan R, Dolphin AC. The increased trafficking of the calcium channel subunit alpha2delta-1 to presynaptic terminals in neuropathic pain is inhibited by the alpha2delta ligand pregabalin. J Neurosci 2009;29:4076–4088. [PubMed: 19339603]
7. Berkefeld H, Sailer CA, Bildl W, Rohde V, Thumfart JO, Eble S, Klugbauer N, Reisinger E, Bischofberger J, Oliver D, Knaus HG, Schulte U, Fakler B. BKCa-Cav channel complexes mediate rapid and localized Ca2+-activated K+ signaling. Science 2006;314:615–620. [PubMed: 17068255]
8. Bilici D, Akpinar E, Gursan N, Dengiz GO, Bilici S, Altas S. Protective effect of T-type calcium channel blocker in histamine-induced paw inflammation in rat. Pharmacol Res 2001;44:527–531. [PubMed: 11735361]
9. Blair NT, Bean BP. Roles of tetrodotoxin (TTX)-sensitive Na+ current, TTX-resistant Na+ current, and Ca2+ current in the action potentials of nociceptive sensory neurons. J Neurosci 2002;22:10277–10290. [PubMed: 12451128]
10. Breese NM, George AC, Pauers LE, Stucky CL. Peripheral inflammation selectively increases TRPV1 function in IB4-positive sensory neurons from adult mouse. Pain 2005;115:37–49. [PubMed: 15836968]

11. Cao YQ, Tsien RW. Different relationship of N- and P/Q-type Ca2+ channels to channel-interacting slots in controlling neurotransmission at cultured hippocampal synapses. J Neurosci 30:4536–4546. [PubMed: 20357104]
12. Cardenas CG, Del Mar LP, Cooper BY, Scroggs RS. 5HT4 receptors couple positively to tetrodotoxin-insensitive sodium channels in a subpopulation of capsaicin-sensitive rat sensory neurons. J Neurosci 1997;17:7181–7189. [PubMed: 9295364]
13. Cardenas CG, Del Mar LP, Scroggs RS. Variation in serotonergic inhibition of calcium channel currents in four types of rat sensory neurons differentiated by membrane properties. J Neurophysiol 1995;74:1870–1879. [PubMed: 8592180]
14. Cardenas CG, Mar LP, Vysokanov AV, Arnold PB, Cardenas LM, Surmeier DJ, Scroggs RS. Serotonergic modulation of hyperpolarization-activated current in acutely isolated rat dorsal root ganglion neurons. J Physiol (Lond) 1999;518:507–523. [PubMed: 10381596]
15. Catterall WA, Perez-Reyes E, Snutch TP, Striessnig J. International Union of Pharmacology. XLVIII. Nomenclature and structure-function relationships of voltage-gated calcium channels. Pharmacol Rev 2005;57:411–425. [PubMed: 16382099]
16. Dang K, Bielefeldt K, Gebhart GF. Gastric ulcers reduce A-type potassium currents in rat gastric sensory ganglion neurons. Am J Physiol Gastrointest Liver Physiol 2004;286:G573–G579. [PubMed: 14525728]
17. Davies A, Hendrich J, Van Minh AT, Wratten J, Douglas L, Dolphin AC. Functional biology of the alpha(2)delta subunits of voltage-gated calcium channels. Trends Pharmacol Sci 2007;28:220–228. [PubMed: 17403543]
18. Djouhri L, Fang X, Okuse K, Wood JN, Berry CM, Lawson SN. The TTX-resistant sodium channel Nav1.8 (SNS/PN3): expression and correlation with membrane properties in rat nociceptive primary afferent neurons. J Physiol 2003;550:739–752. [PubMed: 12794175]
19. Dubreuil AS, Boukhaddaoui H, Desmadryl G, Martinez-Salgado C, Moshourab R, Lewin GR, Carroll P, Valmier J, Scamps F. Role of T-type calcium current in identified D-hair mechanoreceptor neurons studied in vitro. J Neurosci 2004;24:8480–8484. [PubMed: 15456821]
20. Fields RD, Lee PR, Cohen JE. Temporal integration of intracellular Ca2+ signaling networks in regulating gene expression by action potentials. Cell Calcium 2005;37:433–442. [PubMed: 15820391]
21. Flake NM, Bonebreak DB, Gold MS. Estrogen and inflammation increase the excitability of rat temporomandibular joint afferent neurons. J Neurophysiol 2005;93:1585–1597. [PubMed: 15525813]
22. Gold MS, Dastmalchi S, Levine JD. Co-expression of nociceptor properties in dorsal root ganglion neurons from the adult rat *in vitro*. Neuroscience 1996;71:265–275. [PubMed: 8834408]
23. Gold MS, Shuster MJ, Levine JD. Characterization of six voltage-gated K+ currents in adult rat sensory neurons. J Neurophysiol 1996;75:2629–2646. [PubMed: 8793767]
24. Gold MS, Traub RJ. Cutaneous and colonic rat DRG neurons differ with respect to both baseline and PGE2-induced changes in passive and active electrophysiological properties. J Neurophysiol 2004;91:2524–2531. [PubMed: 14736864]
25. Gold MS, Zhang L, Wrigley DL, Traub RJ. Prostaglandin E(2) Modulates TTX-R I(Na) in Rat Colonic Sensory Neurons. J Neurophysiol 2002;88:1512–1522. [PubMed: 12205171]
26. Harriott AM, Dessem D, Gold MS. Inflammation increases the excitability of masseter muscle afferents. Neuroscience. 2006
27. Hogan QH, McCallum JB, Sarantopoulos C, Aason M, Mynlieff M, Kwok W, Bosnjak ZJ. Painful neuropathy decreases membrane calcium current in mammalian primary afferent neurons. Pain 2000;86:43–53. [PubMed: 10779659]
28. Hua XY, Chen P, Fox A, Myers RR. Involvement of cytokines in lipopolysaccharide-induced facilitation of CGRP release from capsaicin-sensitive nerves in the trachea: studies with interleukin-1beta and tumor necrosis factor-alpha. J Neurosci 1996;16:4742–4748. [PubMed: 8764661]
29. Jevtovic-Todorovic V, Todorovic SM. The role of peripheral T-type calcium channels in pain transmission. Cell Calcium 2006;40:197–203. [PubMed: 16777222]

30. Ji RR, Samad TA, Jin SX, Schmoll R, Woolf CJ. p38 MAPK activation by NGF in primary sensory neurons after inflammation increases TRPV1 levels and maintains heat hyperalgesia. Neuron 2002;36:57–68. [PubMed: 12367506]

31. Katz EJ, Gold MS. Inflammatory hyperalgesia: a role for the C-fiber sensory neuron cell body? J Pain 2006;7:170–178. [PubMed: 16516822]

32. Lawson SN, Perry MJ, Prabhakar E, McCarthy PW. Primary sensory neurones: neurofilament, neuropeptides, and conduction velocity. Brain Res Bull 1993;30:239–243. [PubMed: 7681350]

33. Leslie TA, Emson PC, Dowd PM, Woolf CJ. Nerve growth factor contributes to the up-regulation of growth-associated protein 43 and preprotachykinin A messenger RNAs in primary sensory neurons following peripheral inflammation. Neuroscience 1995;67:753–761. [PubMed: 7675201]

34. Li CY, Zhang XL, Matthews EA, Li KW, Kurwa A, Boroujerdi A, Gross J, Gold MS, Dickenson AH, Feng G, Luo ZD. Calcium channel alpha(2)delta(1) subunit mediates spinal hyperexcitability in pain modulation. Pain. 2006

35. Lu SG, Gold MS. Inflammation-induced increase in evoked calcium transients in subpopulations of rat dorsal root ganglion neurons. Neuroscience 2008;153:279–288. [PubMed: 18367340]

36. Lu SG, Zhang X, Gold MS. Intracellular calcium regulation among subpopulations of rat dorsal root ganglion neurons. J Physiol 2006;577:169–190. [PubMed: 16945973]

37. Luo ZD, Chaplan SR, Higuera ES, Sorkin LS, Stauderman KA, Williams ME, Yaksh TL. Upregulation of dorsal root ganglion (alpha)2(delta) calcium channel subunit and its correlation with allodynia in spinal nerve-injured rats. J Neurosci 2001;21:1868–1875. [PubMed: 11245671]

38. McCallum JB, Kwok WM, Mynlieff M, Bosnjak ZJ, Hogan QH. Loss of T-type calcium current in sensory neurons of rats with neuropathic pain. Anesthesiology 2003;98:209–216. [PubMed: 12502999]

39. McCallum JB, Kwok WM, Sapunar D, Fuchs A, Hogan QH. Painful peripheral nerve injury decreases calcium current in axotomized sensory neurons. Anesthesiology 2006;105:160–168. [PubMed: 16810008]

40. Miki K, Zhou QQ, Guo W, Guan Y, Terayama R, Dubner R, Ren K. Changes in gene expression and neuronal phenotype in brain stem pain modulatory circuitry after inflammation. J Neurophysiol 2002;87:750–760. [PubMed: 11826044]

41. Moore BA, Stewart TM, Hill C, Vanner SJ. TNBS ileitis evokes hyperexcitability and changes in ionic membrane properties of nociceptive DRG neurons. Am J Physiol Gastrointest Liver Physiol 2002;282:G1045–G1051. [PubMed: 12016130]

42. Nelson MT, Joksovic PM, Perez-Reyes E, Todorovic SM. The endogenous redox agent L-cysteine induces T-type Ca2+ channel-dependent sensitization of a novel subpopulation of rat peripheral nociceptors. J Neurosci 2005;25:8766–8775. [PubMed: 16177046]

43. Neubert JK, Maidment NT, Matsuka Y, Adelson DW, Kruger L, Spigelman I. Inflammation-induced changes in primary afferent-evoked release of substance P within trigeminal ganglia in vivo. Brain Res 2000;871:181–191. [PubMed: 10899285]

44. Nicol GD, Vasko MR, Evans AR. Prostaglandins suppress an outward potassium current in embryonic rat sensory neurons. J Neurophysiol 1997;77:167–176. [PubMed: 9120557]

45. Petruska JC, Napaporn J, Johnson RD, Gu JG, Cooper BY. Subclassified acutely dissociated cells of rat DRG: histochemistry and patterns of capsaicin-, proton-, and ATP-activated currents. J Neurophysiol 2000;84:2365–2379. [PubMed: 11067979]

46. Scholz A, Gruss M, Vogel W. Properties and functions of calcium-activated K+ channels in small neurones of rat dorsal root ganglion studied in a thin slice preparation. J Physiol 1998;513 ( Pt 1): 55–69. [PubMed: 9782159]

47. Scroggs RS, Fox AP. Calcium current variation between acutely isolated adult rat dorsal root ganglion neurons of different size. Journal of Physiology 1992;445:639–658. [PubMed: 1323671]

48. Scroggs RS, Todorovic SM, Anderson EG, Fox AP. Variation in IH, IIR, and ILEAK between acutely isolated adult rat dorsal root ganglion neurons of different size. J Neurophysiol 1994;71:271–279. [PubMed: 7512627]

49. Westenbroek RE, Byers MR. Up-regulation of class A Ca2+ channels in trigeminal ganglion after pulp exposure. Neuroreport 1999;10:381–385. [PubMed: 10203339]

50. Zamponi GW, Lewis RJ, Todorovic SM, Arneric SP, Snutch TP. Role of voltage-gated calcium channels in ascending pain pathways. Brain Res Rev 2009;60:84–89. [PubMed: 19162069]

51. Zhang XL, Mok LP, Katz EJ, Gold MS. BK(Ca) currents are enriched in a subpopulation of adult rat cutaneous nociceptive dorsal root ganglion neurons. Eur J Neurosci 2010;31:450–462. [PubMed: 20105244]

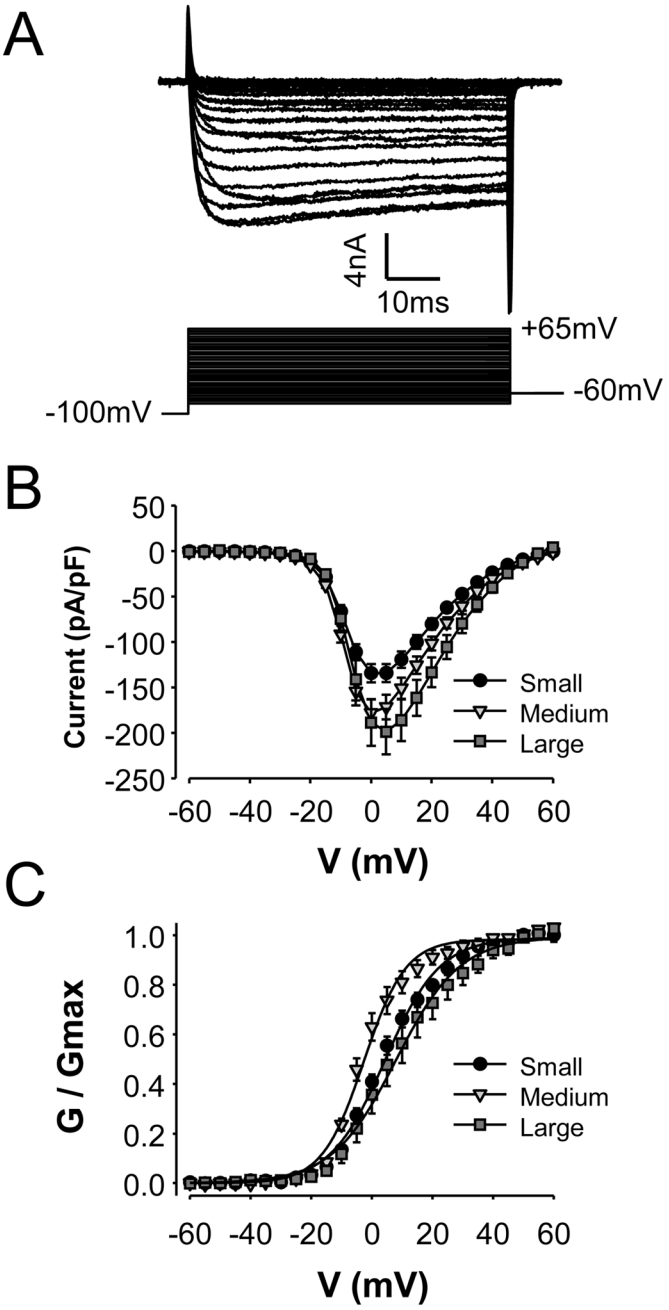


**Figure 1.**

Voltage gated $Ca^{2+}$ currents in cutaneous DRG neurons. **A.** High threshold (HVA) current in a typical small diameter cutaneous afferent had a threshold for activation ~−20 mV and demonstrated little inactivation over a 60 ms voltage step. The protocol used to evoked current is shown below current traces. **B.** Pooled (mean ± SEM) current-voltage (I–V) data from small (n = 33), medium (n = 26) and large (n = 14) diameter cutaneous DRG neurons from control ganglia. Current evoked in each neuron was normalized to the membrane capacitance. **C.** Pooled conductance-voltage (G–V) data generated from instantaneous I–V data (i.e., tail currents) from the same neurons plotted in B.

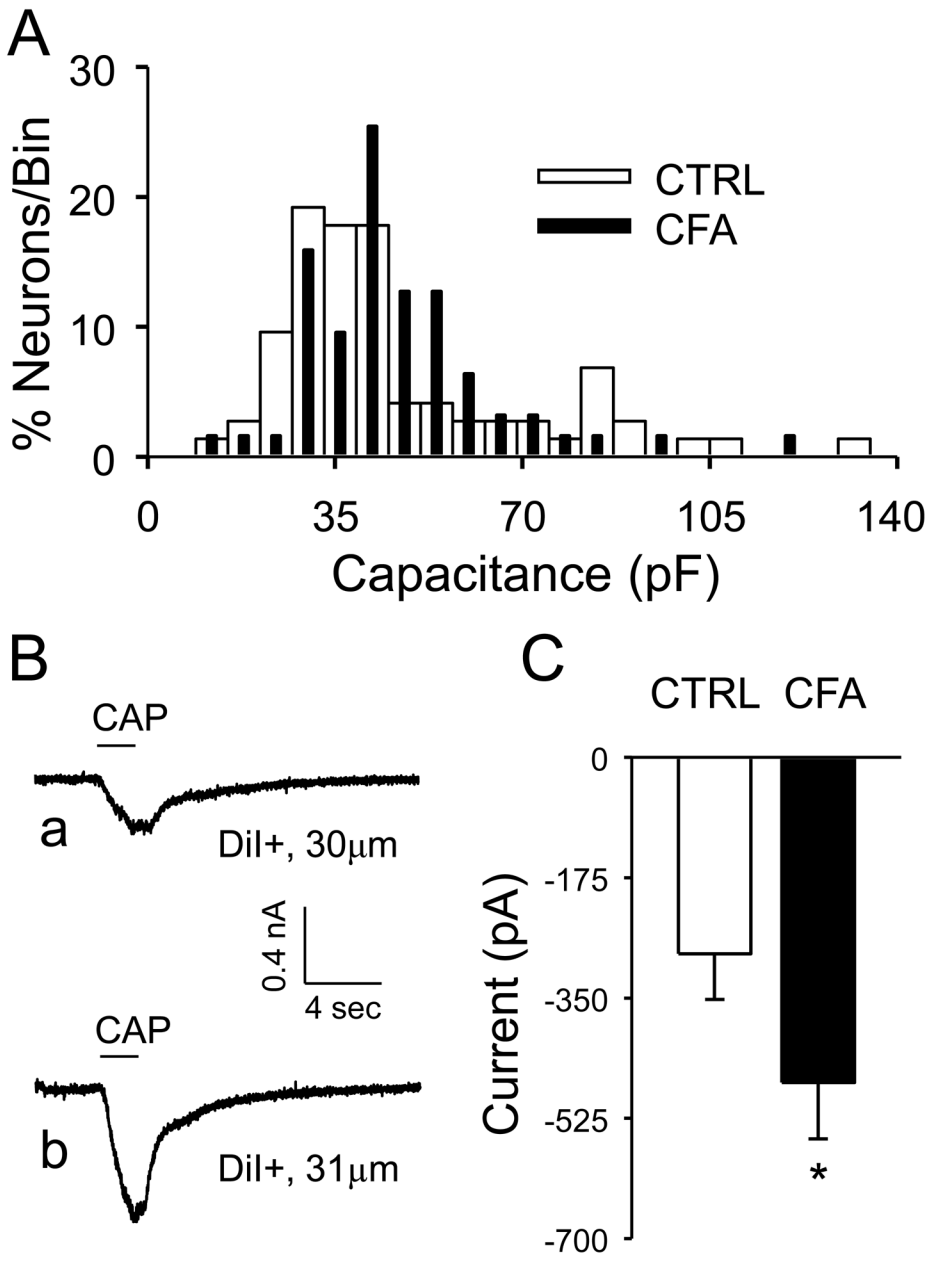


**Figure 2.**

The impact of inflammation on membrane capacitance and capsaicin evoked currents in cutaneous DRG neurons. **A.** Histograms of membrane capacitance for control (CTRL, n = 73) and inflamed (CFA, n = 63) DRG neurons. Bin size is 6 pF. To facilitate comparing the two histograms, they have been plotted together and normalized with respect to the total number of neurons studied in each group. **B.** Typical capsaicin (CAP, 500 nM) evoked responses from a 30 μm diameter control (a) and 31 μm diameter inflamed (b) cutaneous afferent. The holding potential for both current traces was −60 mV. **C.** Pooled peak CAP evoked current from control (CTRL, n = 26) and inflamed (CFA, n = 22) neurons. * is $p < 0.05$ (Students t test).

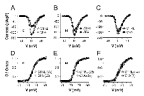

**Figure 3.**

The impact of inflammation on HVA currents in cutaneous DRG neurons. Pooled I–V data for small (S), medium (M) and large (L) diameter cutaneous DRG neurons normalized to cell body capacitance are plotted in panels **A, B** and **C,** respectively. Current density in small and medium, but not large diameter neurons from control (CTRL) rats is significantly larger than that in neurons from inflamed (CFA) rats. Normalized G–V data corresponding to the I–V data plotted in panels **A, B** and **C** are plotted in panels **D, E** and **F**. There was no detectable influence of inflammation on the voltage-dependence of activation in these subpopulations of cutaneous DRG neurons. The number of neurons in each group is indicated in parentheses.

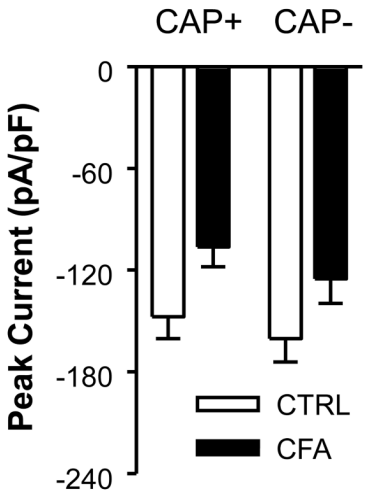


**Figure 4.**

The impact of inflammation on subpopulations of cutaneous DRG neurons defined by capsaicin (CAP) sensitivity. Peak inward HVA current density at 0 mV in CAP sensitive (CAP+) and CAP insensitive (CAP-) cutaneous DRG neurons from control (CTRL) and inflamed (CFA) ganglia. Current density was significantly ($p < 0.01$, two-way ANOVA) larger in control ($n = 63$) than inflamed ($n = 46$) neurons, but there was no difference ($p > 0.05$) between CAP+ ($n = 48$) and CAP– ($n = 61$) neurons with respect to current density, nor was there an interaction ($p > 0.05$) between the impact of inflammation and CAP sensitivity.

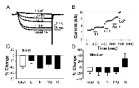

**Figure 5.**

Inflammation decreased multiple types of HVA current in cutaneous DRG neurons. HVA current subtypes were isolated pharmacologically. **A.** HVA current evoked in typical cutaneous afferent from a naïve rat before (Baseline) and after sequential application of nifedipine (Nif, 10 μM) to block L-type currents, ω-conotoxin GVIA (CTx, 200 nM) to block N-type currents, ω-agatoxin IVA (AgTx, 200 nM) to block P/Q-type currents, and cadmium ($Cd^{2+}$, 50 μM) to block residual current (R). **B.** Diary plot of data from afferent shown in A. Pooled data from small (**C**) and medium (**D**) diameter neurons from inflamed rats analyzed as a percent change in current subtype density from that obtained in control neurons.

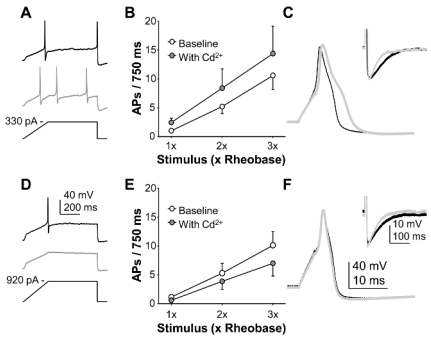


**Figure 6.**

The impact of a decrease in HVA-current on the excitability of cutaneous DRG neurons. Blocking ~40% of HVA current resulted in an increase in the excitability of some small and medium diameter neurons (**A, B** and **C**) and a decrease in the excitability of others (**D, E,** and **F**). Depolarizing current injection in the form of a "ramp and hold" stimulus was used to assess excitability before (black traces) and after (grey traces) the application of $Cd^{2+}$ (5 μM; **A** and **D**). A change in current threshold, action potential threshold, or the number of evoked spikes greater than 2 standard deviations from the baseline response was considered a response to $Cd^{2+}$. The response to suprathreshold stimuli delivered in the form of a "square wave" depolarizing current injection (750 ms) at 1x, 2x and 3x rheobase was increased in neurons excited by $Cd^{2+}$ (**B**, n = 7) and decreased in those inhibited by $Cd^{2+}$ (**E**, n = 8). Changes in excitability were associated with consistent and significant changes in the action potential waveform in neurons excited by $Cd^{2+}$ (**C**), while changes in those inhibited by $Cd^{2+}$ (**F**) were more variable; voltage traces in C and F were typical with baseline traces in black and those obtained in the presence of $Cd^{2+}$ in grey. Insets to each voltage trace are the afterhyperpolarizations on an expanded scale where the action potential is cut off to facilitate inspection of the AHP.

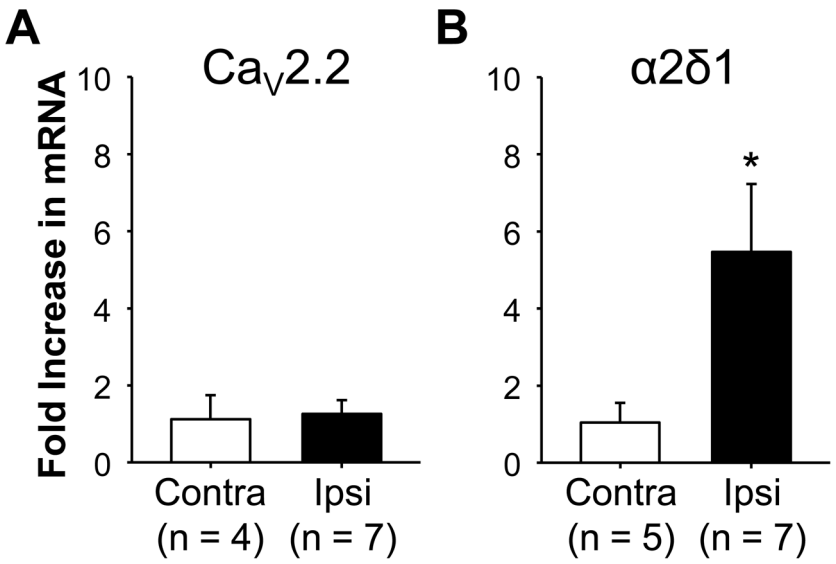


**Figure 7.**

The impact of inflammation of $Ca^{2+}$ channel subunit expression levels. SYBR green was used for semi-quantitative RT-PCR analysis of $Ca_V2.2$ (**A**) and α2δ1 (**B**) subunit expression levels. GAPDH was used as an internal comparator where the ΔΔCT method was used to determine the fold change in subunit expression in ganglia contralateral (Contra) and ispilateral (Ipsi) to the site of inflammation, relative to that in naïve ganglia (n = 4). L4 and L5 ganglia on each side were pooled so that the "n" for each group is an individual rat. While more inflamed ganglia were processed, data were still analyzed with a paired t-test, where * is $p < 0.05$.

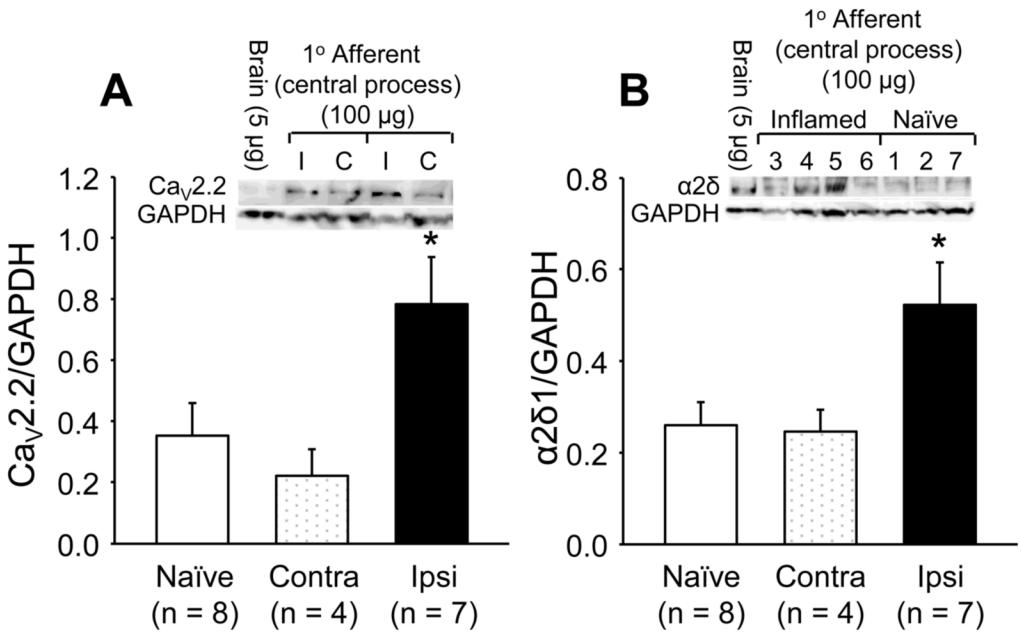


**Figure 8.**

The impact of inflammation on the $Ca^{2+}$ channel subunit levels in the central nerves from L4 and L5 ganglia. Total protein was extracted from the central nerves of L4 and L5 ganglia from naïve rats and from the side contralateral (Contra) and ipsilateral (Ipsi) to the site of inflammation. Band intensity for channel subunits was normalized to that of the loading control (GAPDH). A sample of protein from rat brain was used to normalize data between blots. Pooled data revealed an increase in both $Ca_V2.2$ (**A**) and α2δ1 (**B**) in nerves ispilateral to the site of inflammation ($p < 0.05$, one-way ANOVA).

## Table 1

Parameters of HVA current activation in control and inflamed cutaneous DRG neurons

| | Subpopulation | Gmax ± SE | Slope ± SE | V1/2 ± SE |
|---|---|---|---|---|
| CTRL | Small (33) | 85.9 ± 7.0 | 9.1 ± 0.11 | 4.3 ± 0.33 |
| | Medium (26) | 142.4 ± 13.2 | 6.9 ± 0.21 | −2.6 ± 0.52 |
| | Large (14) | 330.0 ± 44.6 | 10.6 ± 0.18 | 8.0 ± 0.75 |
| | CAP+ (26) | 121.8 ± 12.9 | 3.84 ± 0.15 | −8.20 ± 0.44 |
| | CAP- (37) | 166.6 ± 25.6 | 3.86 ± 0.14 | −7.91 ± 0.47 |
| CFA | Small (22) | 57.44 ± 7.5 | 9.3 ± 0.13 | 6.2 ± 0.61 |
| | Medium (34) | 122.6 ± 8.4 | 7.9 ± 0.11 | 1.4 ± 0.44 |
| | Large (7) | 309.0 ± 45.8 | 11.6 ± 0.36 | 13.0 ± 0.66 |
| | CAP+ (22) | 90.8 ± 11.5 | 4.09 ± 0.17 | −7.18 ± 0.59 |
| | CAP- (24) | 130.1 ± 22.0 | 3.79 ± 0.15 | −7.21 ± 0.64 |

Control neurons included those from both naïve rats and from CFA treated rats contralateral to the site of inflammation. The number of DRG neurons in each subpopulation is in parentheses. Conductance-voltage data for each neuron was fitted with a Boltzmann equation to derive Gmax (maximal conductance), the voltage-dependence of activation (slope) and the potential at which conductance was half of maximal (V1/2). Data were analyzed with a two-way ANOVA to assess the presence of statistically significant main effects associated with inflammation, subpopulation or an interaction between the two. $G_{max}$ was the only parameter in which there were statistically significant differences between groups. There were significant effects associated with both cell body diameter ($p < 0.01$) and capsaicin sensitivity ($p < 0.01$). There was also a significant effect associated with the presence of inflammation when subpopulations were defined by cell body diameter. However, the interaction between cell body diameter and inflammation was not statistically significant. Finally, while there was a significant main effect of cell body diameter on the V1/2 of activation, there was no significant influence of inflammation, nor was there an interaction between the two.

## Table 2

### Distribution of Ca2+ current subtypes in small and medium diameter cutaneous neurons

Data are from small and medium diameter cutaneous DRG neurons from naïve rats and inflamed rats contralateral to the site of inflammation (naïve + contralateral = control) and inflamed rats ipsilateral to the site of inflammation (inflamed). The number of neurons studied in each group is indicated in parenthesis.

| Group | Size | L (% of total) | N (% of total) | P/Q (% of total) |
|---|---|---|---|---|
| Control | Small | 12 ± 2 (n = 12) | 42 ± 3 (n = 13) | 24 ± 3 (n = 7) |
| | Medium | 14 ± 2 (n = 8) | 45 ± 6 (n = 8) | 25 ± 6 (n = 5) |
| Inflamed | Small | 16 ± 2 (n = 12) | 37 ± 3 (n = 12) | 26 ± 1 (n = 11) |
| | Medium | 13 ± 2 (n = 11) | 37 ± 3 (n = 11) | 22 ± 1 (n = 10) |

**Table 3**

The impact of 5 μM $Cd^{2+}$ on the excitability of cutaneous DRG neurons

| Group | $Cd^{2+}$ | AP Thresh (pA) | Current Thresh (mV) | Vrest (mV) | Overshoot (mV) | Duration (ms) | Rise (mV/ms) | Fall (mV/ms) | AHP Mag. (mV) | AHP Decay (ms) |
|---|---|---|---|---|---|---|---|---|---|---|
| Incr. (n = 7) | - | −17.8 ± 1.1 | 330 ± 66 | −64.2 ± 2.2 | 44.4 ± 1.7 | 3.4 ± 0.5 | 85.3 ± 4.4 | 46.4 ± 2.5 | 14.9 ± 1.0 | 243 ± 84 |
| | + | −16.8 ± 0.5 | 277 ± 56* | −59.5 ± 1.9** | 49.5 ± 1.0* | 4.1 ± 0.5** | 96.6 ± 3.4* | 34.5 ± 3.2 | 16.9 ± 1.3 | 136 ± 64 |
| Decr. (n = 8) | - | −15.7 ± 1.4 | 423 ± 126 | −64.2 ± 1.8 | 41 ± 2.9 | 3.1 ± 0.4 | 78.5 ± 7.4 | 49.1 ± 4.1 | 16.0 ± 1.6 | 70.0 ± 4.8 |
| | + | −14.3 ± 1.2 | 423 ± 124 | −64.1 ± 2.1 | 43 ± 2.1 | 3.0 ± 0.2 | 81.0 ± 7.0 | 46.4 ± 4.3 | 15.5 ± 2.1 | 65.0 ± 4.8 |

Data are from small and medium diameter cutaneous DRG neurons grouped as a function of whether $Cd^{2+}$ resulted in an increase (Incr.) or decrease (Decr.) in excitability. Data was collected before (−) and after (+) application of $Cd^{2+}$. Pooled data are presented as mean ± SEM where the presence of a significant change in each parameter was assessed with a paired t-test.

* is $p < 0.05$ and

** is $p < 0.01$.

AP Thresh is action potential threshold assessed with ramp and hold stimulus. Current threshold is the magnitude of the current injection corresponding to AP Threshold. Vrest is resting membrane potential. Overshoot is AP amplitude above 0 mV. Duration is AP duration at 0 mV. Rise is the maximum rate of AP rise. Fall is the maximum rate of AP fall. AHP Mag is the magnitude of the afterhyperpolarization following the AP. AHP decay is the time constant for the decay phase of the AHP.